MPMI Vol. 35, No. 8, 2022, pp. 639–649, https://doi.org/10.1094/MPMI-01-22-0011-TA

TECHNICAL ADVANCE

Development of an Experimental Approach to Achieve Spatially Resolved Plant Root-Associated Metaproteomics Using an Agar-Plate System

Manasa R. Appidi,[1,2] Amber N. Bible,[1] Dana L. Carper,[1] Sara S. Jawdy,[1] Richard J. Giannone,[1] Robert L. Hettich,[1] Jennifer Morrell-Falvey,[1] and Paul E. Abraham[1,†]

[1] Biosciences Division, Oak Ridge National Laboratory, Oak Ridge, TN 37831, U.S.A.
[2] Department of Genome Science and Technology, University of Tennessee-Knoxville, Knoxville, TN 37996, U.S.A.

Accepted for publication 26 March 2022.

Plant–microbe interactions in the rhizosphere play a vital role in plant health and productivity. The composition and function of root-associated microbiomes is strongly influenced by their surrounding environment, which is often customized by their host. How microbiomes change with respect to space and time across plant roots remains poorly understood, and methodologies that facilitate spatiotemporal metaproteomic studies of root-associated microbiomes are yet to be realized. Here, we developed a method that provides spatially resolved metaproteome measurements along plant roots embedded in agar-plate culture systems, which have long been used to study plants. Spatially defined agar "plugs" of interest were excised and subsequently processed using a novel peptide extraction method prior to metaproteomics, which was used to infer both microbial community composition and function. As a proof-of-principle, a previously studied 10-member community constructed from a *Populus* root system was grown in an agar plate with a 3-week-old *Populus trichocarpa* plant. Metaproteomics was performed across two time points (24 and 48 h) for three distinct locations (root base, root tip, and a region distant from the root). The spatial resolution of these measurements provides evidence that microbiome composition and expression changes across the plant root interface. Interrogation of the individual microbial proteomes revealed functional profiles related to their behavioral associations with the plant root, in which chemotaxis and augmented metabolism likely supported predominance of the most abundant member. This study demonstrated a novel peptide extraction method for studying plant agar-plate culture systems, which was previously unsuitable for (meta)proteomic measurements.

Keywords: agar-plate system, agar removal, constructed microbial community, metaproteomics, plant-associated microbes, reductionist approach, rhizosphere microbiome, spatially resolved microbiomes

Plants are continually interacting with microbes, some of which benefit the host while others thrive at the host's expense (Schirawski and Perlin 2018). Microbes can be found across several regions of the plant, including the phyllosphere (above the ground), endosphere (inside plant tissues both above- and belowground), and rhizosphere (belowground region surrounding the roots) (Vandenkoornhuyse et al. 2015). There are many interacting factors that ultimately shape the composition of the associated microbiomes, with the relative success of microbial establishment and persistence largely dependent on how well an individual competes for host-mediated resources. Across the plant root system, the deposition of a complex mixture of secondary metabolites, amino acids, secreted enzymes, and cell lysates has been shown to play a role in shaping microbial communities (Bais et al. 2008; Dennis et al. 2010; Doornbos et al. 2012) yet how microbiomes emerge and function along the plant root axis remains poorly understood.

In general, complex plant–microbe systems can be studied using either a holistic or reductionist approach. Characterizing biological systems with a holistic approach generates a more realistic assessment but with less control over the many biotic and abiotic factors influencing experimental observations. Reductionist approaches, on the other hand, offer more control but observed outcomes may be less applicable to our understanding of natural systems because nature's many complexities are not fully considered. As such, research efforts working to bridge the holistic-reductionist divide are crucial to advancing our understanding of these complex biological systems (O'Banion et al. 2020; Tecon et al. 2019). By first building a detailed understanding of relatively simple biological

†Corresponding author: P. E. Abraham; abrahampe@ornl.gov

Funding: This research was sponsored by the Genomic Science Program, U.S. Department of Energy, Office of Science, Biological and Environmental Research, as part of the Plant-Microbe Interfaces Scientific Focus Area. Oak Ridge National Laboratory is managed by UT-Battelle, LLC, for the U.S. Department of Energy under contract DE-AC05-00OR22725.

e-Xtra: Supplementary material is available online.

The author(s) declare no conflict of interest.

systems, high predictive power can eventually be achieved through combining different abiotic or biotic factors to recapitulate natural environments. As more complex systems are studied, certain principles governing plant–microbe interactions are expected to become more or less relevant, and these realizations will begin to uncover higher-order interactions influenced by experimental designs.

In the absence of plant hosts, experimental manipulations of nutrient availability on microbial community assemblage and compositional trajectory are often performed via serial dilution (Goldford et al. 2018; Shrestha et al. 2021; Wang et al. 2021). The outcome of these experimental manipulations can uncover how different compositions of microbes may coexist or competitively exclude one another based on resource availability (Mello et al. 2016; Shrestha et al. 2021). Understanding the fundamental implications of resource competition on microbial community assembly and functions along a plant root is important but is currently limited by methodological challenges.

Plant root-associated microbiomes are most effectively characterized by extraction methods that aim to maximize depth and coverage of the microbial biomass without disrupting the plant host tissue to minimize measurement interference (Knief et al. 2012). Of course, studies aiming to interrogate endophytic microbes within plant tissue becomes significantly more difficult due to competing plant biomass and, therefore, require more elaborate extraction procedures not described here (Nobori et al. 2020). Current methods to extract and subsequently characterize root-associated microbes are most often achieved via physical removal of microbial cells from the surface of the root via washing with or without sonication procedures (Hirsch and Mauchline 2012). It should be expected that the success of these approaches will be influenced by the overall amount of microbial biomass available for characterization; therefore, overall root size and microbial growth and activity are important factors that must be considered.

It is now well known that different plant species select for distinct microbiome communities along their root systems through differences in rhizodeposition of resources (Ruger et al. 2021). The dynamic nature of root growth and development leads to a continuous temporal and spatial change in the amount and composition of rhizodeposits and, in turn, dynamic changes in the local microbiome compositions and functional activity (Bonkowski et al. 2021). For example, at root tips, plants may slough off cells and secrete mucilage whereas, further up the root, exudates are passively released via root hair cells (Iijima et al. 2000; Knee et al. 2001; Walker et al. 2003). Currently, extraction methodologies that facilitate spatiotemporal characterization of root-associated microbiomes are yet to be realized.

Plant agar-plate culture systems are widely used (Ramirez-Villacis et al. 2020) and would offer an appropriate platform for laboratory-controlled manipulation of root-associated microbiome assemblage to understand the influence of nutrient availability along the root axis. The semisolid agar matrix facilitates microbial movement and allows microbes to form communities based on the variable chemical environments surrounding the root. However, a method to spatially extract and characterize root-associated microbiomes at a molecular level using this agar-based platform has yet to be developed. Here, we describe and ground-truth a method by which microbiomes can be extracted from an agar matrix. In particular, we focus on an extraction method designed for mass spectrometry-based metaproteomics because it provides accurate estimates of both microbial relative abundances and functional activity (Kleiner et al. 2017; Long et al. 2020). We utilized a synthetic community (SynCom) consisting of 10 taxonomically diverse bacterial strains to characterize the spontaneous assembly and function of a *Populus trichocarpa* root-associated microbiome. The method described herein is easy to implement and facilitates spatially resolved metaproteomics of microbial communities along the plant root axis. More broadly, this method can be used to characterize a myriad of biological systems employing agar-based culture systems.

RESULTS AND DISCUSSION

A novel approach to extract and characterize root-associated microbiomes using metaproteomics.

Currently, extraction methods employing washing are used for metaproteomic characterization of root-associated microbiomes (Bao et al. 2014; Knief et al. 2012). Here, we evaluated the performance of a detergent-based wash solution (i.e., root wash) and compared it with the novel peptide extraction method from agar (i.e., agar extraction) (discussed below). For both methods, high-resolution mass spectrometry-based metaproteomics was employed to characterize the microbiome directly associated with a 3-week-old *P. trichocarpa* root surface 48 h postinoculation with a 10-member SynCom.

We found large differences in the number of total proteins identified and the plant root protein contamination between the two methods. For the root wash method, we identified 5,776 proteins, and approximately 37% (Fig. 1A and B) of these were from *Populus* roots. Although metaproteomics has been applied in several root-related studies (Bao et al. 2014; Hara et al. 2019; Mattarozzi et al. 2017, 2020), to our knowledge, there are no previous measurements that could be used to appropriately benchmark these results. Moreover, comparing these results to other studies is not trivial given that microbiome complexity (composition and function) is context specific. Nevertheless, qualitatively, these measurements achieved a similar depth in the number of organisms and proteins identified when compared with a measurement performed on a cell pellet obtained from the inoculum used for SynCom inoculation (Supplementary Fig. S1A). In general, this comparison suggests that the amount of biomass available for metaproteomic measurements in this plant–microbe root system was not a limitation.

The ability to selectively extract and characterize microbiomes from the agar surrounding the whole plant root system is expected to improve the depth and context of metaproteomic measurements for three major reasons: (i) avoiding an extraction directly from the root surface is expected to reduce the number of identified plant proteins; (ii) the amount of microbial biomass is not limited by root surface area; and (iii) spatial sampling provides locational context which, if varied across the root or nutritional gradients, enables the sampling of potential niche members or functional signatures that would otherwise be missed. Therefore, we compared the results from the root wash (whole root wash, 48 h) to an experimentally paired agar plug excised from the surrounding root (whole root plug, 48 h). Indeed, the overall metaproteomics depth achieved by this novel extraction method far surpassed the washing method alone (approximately 53% gain in protein IDs). In total, the extract and measurement from the collected whole root agar plug resulted in a higher number of proteins identified (8,853 proteins) with a notably lower percentage of plant proteins (3.3%) observed (Fig. 1A and B). Additionally, approximately 90% of the proteins identified by the root wash method overlapped with the associated whole root agar plug.

Although the overall depth of the metaproteome coverage improved, the microbiome composition is expected to be spatially influenced by the plant root system. Therefore, we used

metaproteomics to estimate relative microbial biomass amounts (Kleiner et al. 2017) (Fig. 1C; Supplementary Table S1) and performed an analysis of variance (ANOVA) test to assess the similarity of composition and relative abundance of organisms between the microbiome directly associated with the plant root system (root wash) and the microbiome in agar immediately surrounding the root (agar extraction). For this particular comparison, the overall microbiome composition was statistically unchanged ($P = 1$). Individually, however, a relatively low-abundance member (*Rhizobium* sp. strain CF142) did slightly vary in abundance between the two extractions (Supplementary Table S2). The observed change in the abundance of this particular microbe could be indicative of a biological deviation from the averaged microbial population directly interacting with the root surface; however, an alternative explanation is that the increased metaproteomics depth—resulting from reduced plant root protein "contamination"—improved the accuracy of the estimated average composition of root-associated microbes. Furthermore, the agar-plug extraction method increased measurement reproducibility, as demonstrated by derived organism ratios across replicates (Fig. 1C). Regardless, the estimated microbial compositions are nearly indistinguishable between the two approaches but, more importantly, the success of the agar-plug extraction method provides exciting new opportunities to achieve spatially resolved metaproteomics along the plant root axis.

Spatially resolved metaproteomics along the plant root axis.

Spatiotemporal patterns of microbiome assembly, organization, and function are expected to exist along the plant root axis (Bonkowski et al. 2021; Munoz-Ucros et al. 2021) yet it remains unknown how, why, when, and where particular microbes successfully compete for plant-derived nutrients. Therefore, the ability to obtain high-quality metaproteomic datasets from agar motivated us to characterize the temporal and spatial assembly of the SynCom community along the *P. trichocarpa* plant root system.

Prior to studying the assembly and function of the SynCom along the plant root axis, we employed the newly developed extraction method to assess community composition changes between 0-, 24-, and 48-h time points in the absence of the plant (control) when allowed to grow in a modified growth media (discussed below). To support early microbial growth and motility, the Hoagland's growth media commonly used for growing plants was supplemented with 0.1% sucrose and 0.3% agarose (Fig. 2). On average, the number of identified proteins increased across the time points (Supplementary Fig. S1B), and this is likely a result of increases in available biomass as well as changes in the metaproteome expression profiles. Importantly, the estimated starting SynCom composition was statistically unchanged when extracted from the inoculum or using the newly developed agar extraction method ($P = 1$) (Supplementary Fig. S2). Based on a permutational multivariate analysis of

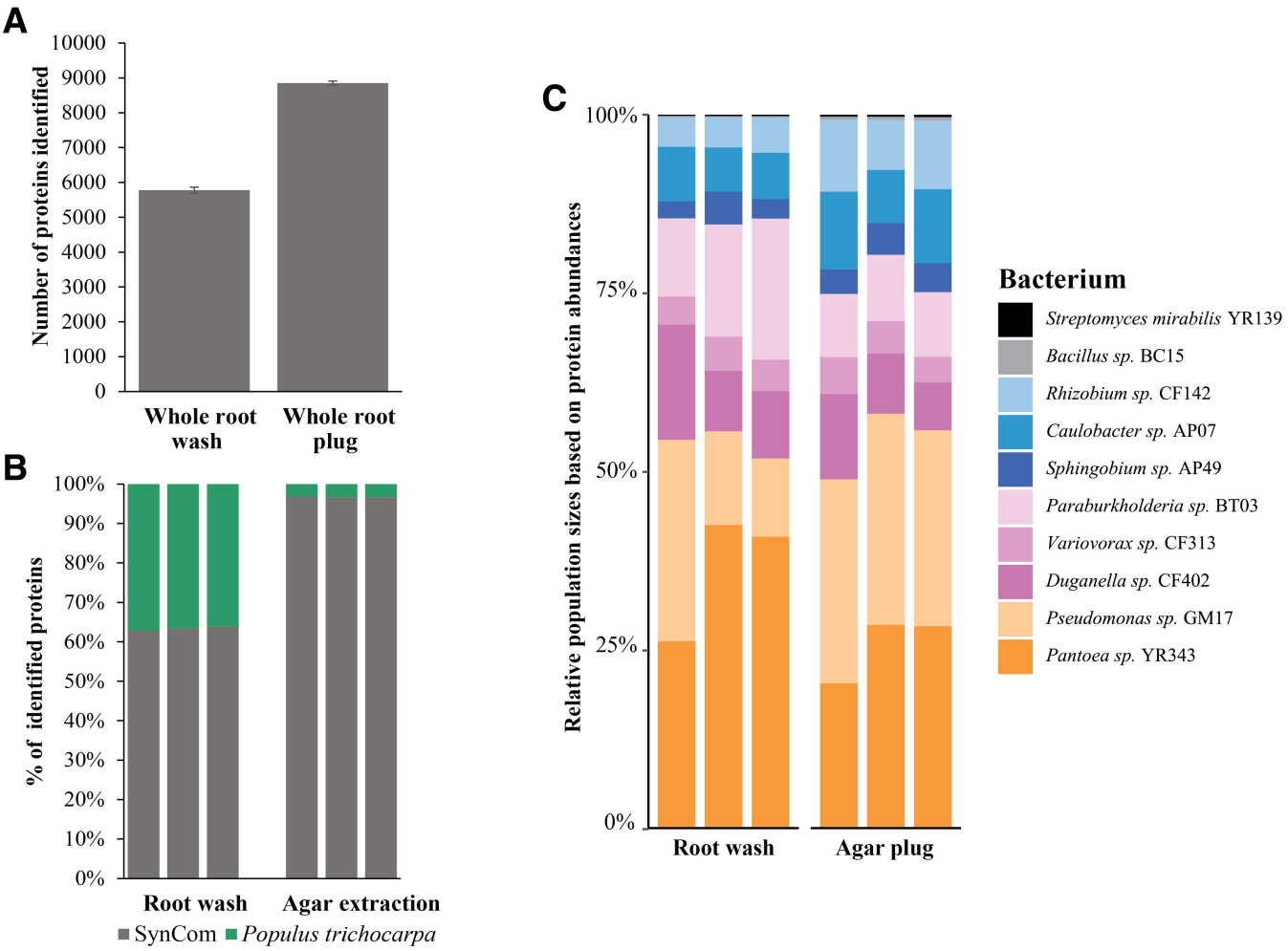

Fig. 1. Proteins extracted from root-associated microbiomes using different extraction methods for plant-agar samples at 48 h. **A,** Average number of proteins identified ($n = 3$). Error bars represent standard error of mean. **B,** Percentage of proteins identified for synthetic community (SynCom) and *Populus trichocarpa*. **C,** Relative organism abundances for the bacterial strains using their summed protein abundances.

variance (PERMANOVA) ($P = 0.004$), the overall community composition changed significantly in control across the 48-h period (Fig. 2). Individually, nine members exhibited a significant change in their relative abundance between the time points (Supplementary Table S3). In this particular environment (i.e., media sans *P. trichocarpa*), *Pantoea* sp. strain YR343 increased in relative abundance to become a dominant member of the SynCom at the 24-h time point. However, this was no longer apparent at the 48-h time point, whereby *Caulobacter* sp. strain AP07 and *Rhizobium* sp. strain CF142 became the two most dominant members.

The same starting SynCom solution was then applied to a 3-week-old *P. trichocarpa* root system and allowed to grow for 48 h. To assess the influence of the plant root system on SynCom assembly, agar plugs were excised to obtain three spatial measurements: root tip, root base, and a region distant from the plant root system. Each discrete location was characterized at 24- and 48-h time points (Supplementary Table S1). Similar to the no-plant SynCom measurements, the average number of identified proteins generally increased from the 24- to 48-h time point and proteins identified per sample group ranged from 2,500 to 3,500 across the sample groups (Supplementary Fig. S1C). Overall, biological reproducibility between agar was high (average Pearson correlation coefficients of approximately 0.89).

To assess the effect of plant, spatial location, and time on the SynCom, PERMANOVA was performed on Euclidean distances using the metaproteomics data collected. Overall, the plant root system had the greatest influence on the measured microbiomes (50%), followed by the interaction between plant and time (24%), and time (14%) (Fig. 3A; Supplementary Table S4). Intriguingly, there was a notable difference between microbiome compositions in the control agar plug at the 48-h time point and the region distant from the root at the 48-h time point. Both sample groups were expected to have similarly assembled communities at the 48-h time point because the influence of plant nutrients was absent or presumably lacking. Given the observed differences in microbiome composition, this result suggests that the plant root's zone of influence reaches significantly outward to the edges (approximately 3 to 4 cm from nearest root) of the plant-agar culture plates. Here, the root-associated microbiome composition largely favored the abundance of *Pantoea* sp. strain YR343, with its relative abundances increasing in the SynCom along the root system and the greatest abundance being observed at the root base. Additionally, four individual members of the SynCom had relative abundances that were significantly changing across the plant root axis (Supplementary Table S5). For example, *Rhizobium* sp. strain CF142 became the second most dominant member at the root tip at the 48-h time point (Fig. 2).

Detecting functional changes in microbial activity along the plant root axis.

Beyond estimating microbiome compositions, metaproteomics can improve our understanding of how a distinct subset of SynCom members was able to grow and thrive along the plant root system in this particular environment (Mattarozzi et al. 2017; Renu et al. 2019). To this end, we interrogated the proteome data of *Pantoea* sp. strain YR343, the most dominant plant-root-associated microbe, to assess its functional profile across the 24- and 48-h time points with and without the plant

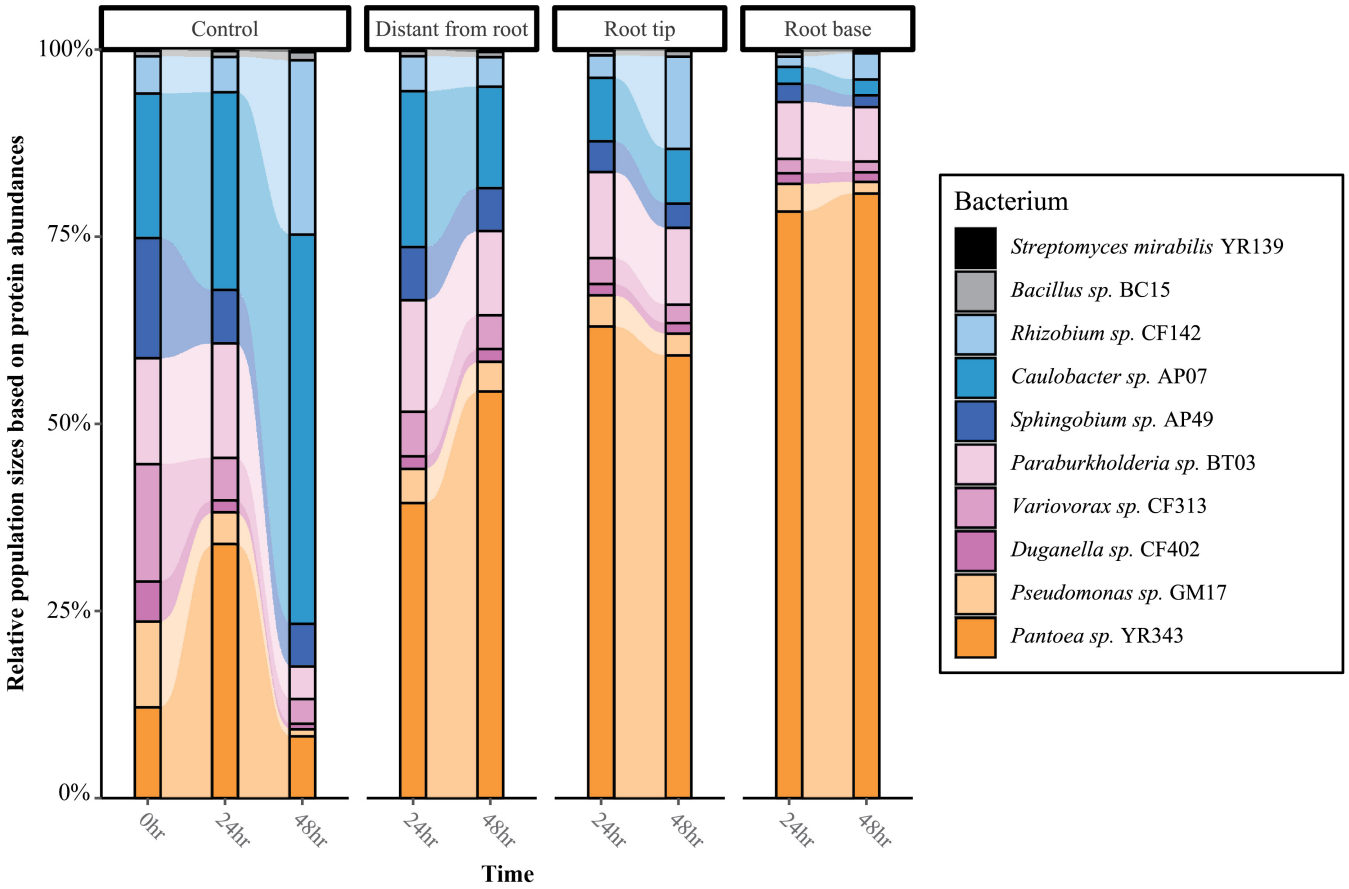

Fig. 2. Assessment of microbial relative population sizes based on their summed protein abundances. Averaged organism relative abundances ($n = 3$) are illustrated for identified microbes in control plugs at 0, 24, and 48 h and three discrete locations surrounding the plant root system (root tip and base and a region distant from the root) at 24- and 48-h time points.

root system. Altogether, this analysis included 1,803 proteins representing approximately 37% of the encoded *Pantoea* sp. strain YR343 reference proteome. Importantly, this amount of proteome coverage is similar to what was achieved in prior proteomic studies of this individual bacteria (Estenson et al. 2018; Kumar et al. 2020).

Factors influencing microbiome composition were similar to those affecting proteome expression of *Pantoea* sp. strain YR343. PERMANOVA results indicate that the plant root system has a major influence (66%) on proteome expression, followed by the interaction of plant and time (17%) and time (8%) (Fig. 3B; Supplementary Table S4). To identify the differentially abundant proteins in *Pantoea* spp. across the measured proteomes, an ANOVA test was performed; 1,720 proteins were determined to have a significant difference in relative protein abundance across the sample groups (P value ≤ 0.05). One-way hierarchical clustering was performed providing a comprehensive picture of protein regulation across the experimental conditions (Fig. 4). In total, four major clusters were observed. The cluster with the most membership (cluster 3; 566 proteins) consists of proteins with increased relative abundance in all plant root extractions when compared with the control samples at the 24- and 48-h time points. In other words, cluster 3 represents proteins upregulated in relative abundance in the presence of the 3-week-old *P. trichocarpa* root system. A gene ontology (GO) enrichment analysis on the proteins in cluster 3 revealed 36 overrepresented GO terms for biological processes and molecular functions (Supplementary Table S6). These GO terms included but were not limited to ion binding, cell motility, transport, response to stress, membrane organization, generation of precursor metabolites, and energy. At a high functional level, these molecular processes explain how *Pantoea* sp. strain YR343 responds to the plant root chemical environment where it competes for available resources through overexpression of several motility-related proteins such as methyl-accepting chemotaxis proteins, response regulator proteins with CheY-like receiver domains, chemotaxis signal transduction proteins, and reprogramming its growth and metabolic activities.

Conclusions.

Functional genomic measurements for plant-root-associated microbiomes are often challenged by the performance of available extraction methods (Tartaglia et al. 2020). In nature, plant root systems are surrounded by complex soil chemistries and physical properties that will vary by biome (e.g., tropical, temperate, or grassland) (Chiu et al. 2002; Shrestha and Kafle 2020). In order to effectively extract the limited amount of available microbiome DNA, mRNA, or proteins, extraction protocols are often tailormade to the characteristics of the environmental matrix (Chourey et al. 2010; Sharma et al. 2012). For example, soils sustaining plants in natural forests or agricultural crops with higher humic acid amounts can be problematic for protein extraction methods (Mandalakis et al. 2018; Qian and Hettich 2017). When successful, these holistic approaches provide necessary information for improving our understanding of plant–microbe interactions occurring in natural ecosystems by considering the interdependencies of environment, function, and genotype (Bona et al. 2019; Renu et al. 2019). Unfortunately, the complexity of these systems is often too high to answer questions related to how microbiome communities and functions are altered by plant root rhizodeposition at certain points in space or time.

In order to address knowledge gaps precluded by too much complexity, experimental representation of biological systems is instead refined to key parameters and their interplay. For plant-microbe interactions, these reductionist approaches are performed using a variety of artificial components (Hemkemeyer et al. 2014; Poole 2017) or engineered laboratory systems and permit us to answer important questions currently unobtainable in natural ecosystems (Yee et al. 2021; Zengler et al. 2019). For example, the widely used plant-agar system offers a well-controlled platform, with low-to-medium complexity, that would

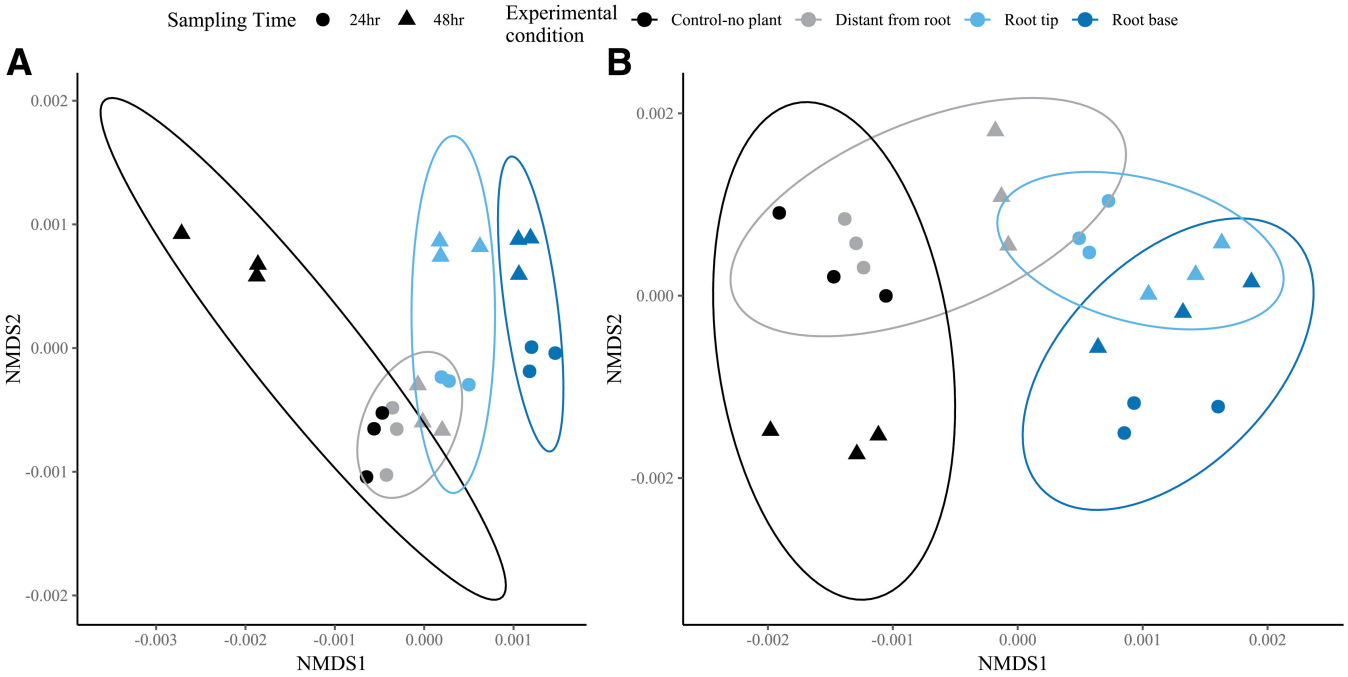

Fig. 3. Association with plant shows higher variation in proteome expression of synthetic community. **A,** Nonmetric multidimensional scaling (NMDS) plot based on Euclidean distances of 10-member proteomics data showed higher variation is observed in relation to association with the plant (permutational multivariate analysis of variance [PERMANOVA], $R^2 = 50.2\%$) followed by the interaction between the relation to plant and time (24%) and then time (13.9%). **B,** NMDS plot based on Euclidean distances of *Pantoea* sp. strain YR343 proteomics data showed that higher variation is observed in relation to association with plant (PERMANOVA, $R^2 = 65.7\%$) followed by the interaction between the relation to plant and time (17.1%) and then time (8.4%).

permit us to answer several important questions. How do microbiome communities assemble in the presence of a plant root system? How does composition and function change along the plant root system at certain points in time and space? Does assembly and maintenance of root-associated microbiomes observed with a specific plant genotype remain the same for other host genotypes? Unfortunately, a method to assess spatiotemporal plant–microbe interactions along the root system in plant-agar systems at a molecular level is yet to be realized.

In order to address this technical limitation, we developed a novel peptide extraction method for high-resolution metaproteome characterization of plant-agar systems. After inoculating

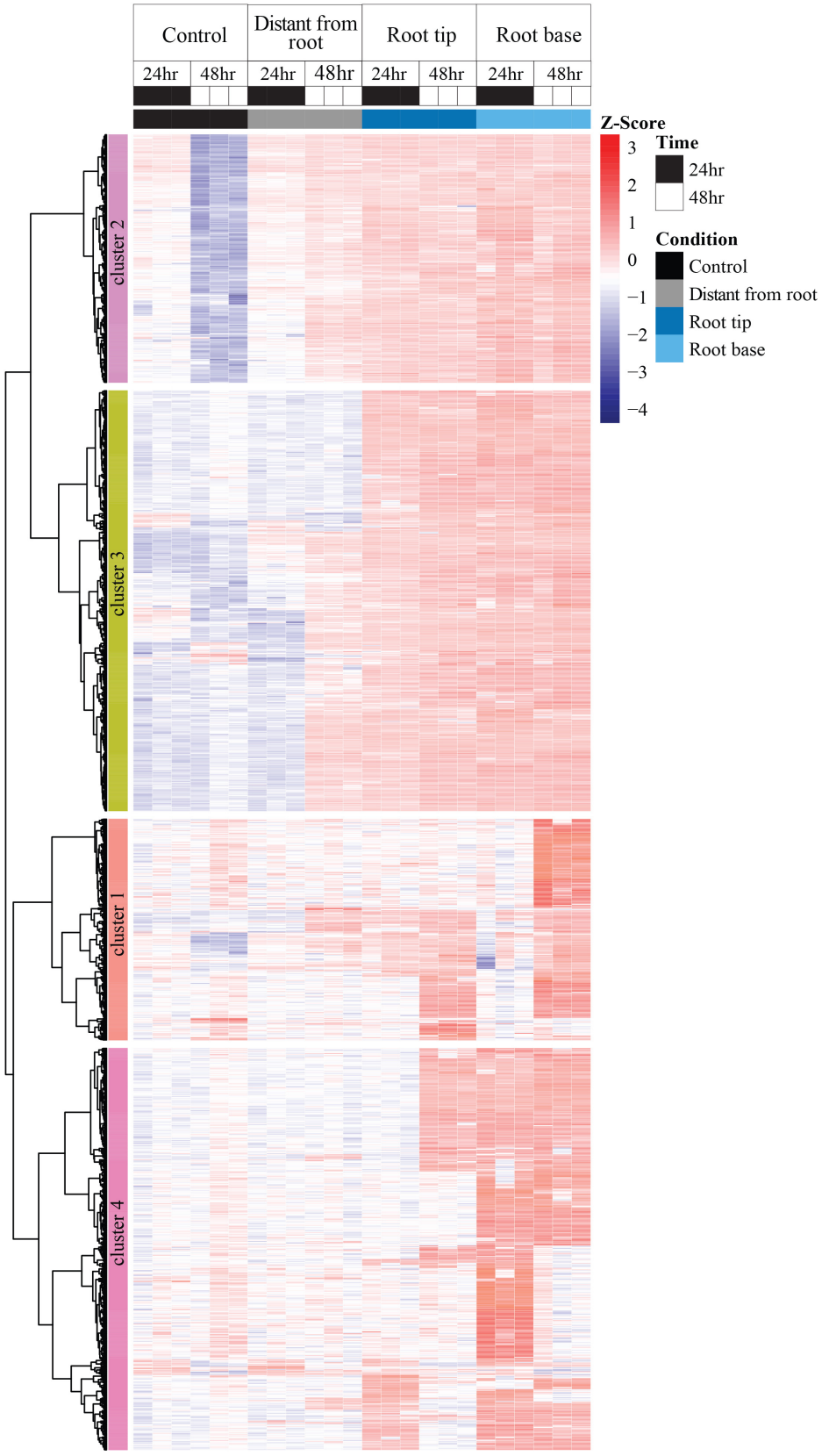

Fig. 4. Hierarchical clustering results for *Pantoea* sp. strain YR343. One-way hierarchical clustering (rows = Euclidean distances) of Z-scores of $\log_2$-transformed protein abundances for significantly regulated proteins (multiple-sample test analysis of variance was performed in Perseus software, permutation-based false discovery rate < 0.05; number of randomizations = 250) across experimental conditions for *Pantoea* sp. strain YR343 revealed four major clusters of proteins.

a 3-week-old *Populus* plant root system with a 10-member SynCom and allowing growth for a 48-h period, we compared the performance (number of proteins identified) and resulting estimates of organism relative abundances between a root wash method and the newly developed agar extraction method. When comparing the two methods, we observed statistically unchanged estimates of microbiome composition and deeper metaproteome measurements (approximately 53% gain in protein identifications) for the agar extraction method, supporting the utility of the agar extraction method for whole-root characterization of microbiomes. More importantly, we demonstrated that this method affords new capabilities in sampling the spatial composition and function of root-associated microbiomes along the plant root axis.

For this particular plant–microbe biological system, substantial changes in composition and function were observed from the root base to the root tip, and even at a region distant from the plant root system. These findings have significant implications in our understanding of how microbiomes respond to plant rhizodeposition and how nutrient availability can affect the nature of microbiome assembly in different niche environments, particularly those associated with *Populus* spp. In fact, this study was designed to complement a previous work that used the same 10-member SynCom but assessed microbiome assembly in a liquid culture environment with rich or minimal media (Shrestha et al. 2021). The high-level observation that the same 10-member SynCom forms different assemblies across varying methodological frameworks is quite intriguing because we can now work to identify rules of assembly, and understanding these rules will give us greater insight into predicting how microbiomes assemble in different environments. More broadly, we anticipate that this novel extraction approach will benefit other soft-agar plate studies that study nutrient exchange among microbes (Abreu and Taga 2016).

Quite surprisingly, we recognized that the 10-member SynCom community assembled in this study is nearly identical in composition to that observed in a previously studied clay soil matrix that was measured using 16S ribosomal RNA gene amplicon sequencing (Carper et al. 2021). The major difference between the two experiments is that it took 21 or 2 days to form nearly identical communities in potted soil or plant-agar, respectively. We posit that environmental matrix properties such as hydration levels, which affect the diffusion of plant rhizodeposits and microbial mobility, resulted in these temporal differences. Although we anticipate that community assembly will become more distinct between the plant-agar system and more natural soils, the relatedness with clay soil matrix addresses concerns about the plant-agar system being too artificial.

MATERIALS AND METHODS

Preparation of plants, bacterial cultures, and a SynCom.

P. trichocarpa (genotype B819) shoot tips were cut from greenhouse-grown plants and sterilized for 4 h by rotating in a 50-ml solution of 1× Murashige-Skoog (MS) basal media with vitamins and glycine (Caisson) and 5% plant-preservative mixture (PPM) (Plant Cell Technology). Once sterilized, the shoot tips were rinsed in sterile H_2O and rooted in a growth chamber (16-h daylength, 15.6 μmol full-spectrum LED) in 1× MS basal medium with vitamins and glycine (Caisson), 0.05% morpholineethanesulfonic acid hydrate (Sigma-Aldrich), 3% sucrose, 0.1% PPM (Plant Cell Technology), 0.5% activated charcoal (Sigma-Aldrich), and 0.18% Gelzan (Plant Media) to establish stock plants. After rooting and growing to an adequate size, axenic shoot tips were subcultured from stock plants and placed into new enclosed containers of the tissue culture media described above and grown for 3 weeks in the same growth chamber until rooted.

A previously described microbial SynCom consisting of 10 bacterial strains previously isolated from *P. deltoides* root systems were used (Shrestha et al. 2021; Wang et al. 2021). Bacterial strains used in this SynCom were *Bacillus* sp. strain BC15, *Caulobacter* sp. strain AP07, *Duganella* sp. strain CF402, *Pantoea* sp. strain YR343, *Paraburkholderia* sp. strain BT03, *Pseudomonas* sp. strain GM17, *Rhizobium* sp. strain CF142, *Sphingobium* sp. strain AP49, *Streptomyces* sp. strain YR139, and *Variovorax* sp. strain CF313 (Aufrecht et al. 2018; Bible et al. 2016; Blair et al. 2018; Brown et al. 2012; Carper et al. 2021; Hasim et al. 2018; Levy et al. 2018; Schaefer et al. 2013; Timm et al. 2016). Overnight cultures of all 10 bacterial strains were grown in R2A liquid media (Teknova) (Reasoner and Geldreich 1985) at 28°C and 250 rpm. For the SynCom, the 10 bacterial cultures were normalized to an optical density at 600 nm of 2.40 and equal volumes of the 10 cultures were combined to generate the bacterial inoculum used in these studies.

Plant-agar culture growth conditions.

Rooted *P. trichocarpa* plants were removed from initial growth media (which leaves the plant roots mostly clean with no debris) and roots were submerged in 25 ml of 1/4× Hoagland's media (Hoagland modified basal salt mixture; PhytoTech Labs) supplemented with 0.1% sucrose, 0.3% agarose, and the SynCom community at a concentration of approximately 10^7 cells/ml in a sterile Petri dish. Each plant-agar culture was incubated for 24 h ($n = 3$) or 48 h ($n = 3$) in a sterile plastic container to maintain humidity at 28°C in growth chambers with 16-h days alongside agar control plates ($n = 3$ for 24 and 48 h) that were similarly produced but lacked plant hosts (Fig. 5A).

Extracting microbiomes directly associated with the plant root system for metaproteomics.

To characterize microbiomes directly associated with the root surface, plant roots (biological triplicates) were excised with a sterile scalpel and transferred to Eppendorf tubes and washed in 300 μl of sodium dodecyl sulfate (SDS) lysis buffer (4% SDS [Sigma-Aldrich] in 100 mM Tris, pH 8.0) by vortexing gently to liberate microbial cells bound to roots. The roots were removed, and crude lysate suspensions were sonicated (30% amplitude, 10-s pulse with 10-s rest, 2-min total pulse time) (Branson digital sonifier) and boiled at 90°C for 10 min to complete microbial lysis. The cell lysates were centrifuged at 21,000 × *g* for 10 min at room temperature to remove any cell debris. Samples were reduced by adjusting to 10 mM dithiothreitol (Sigma Life Science) by incubating at 90°C for 10 min, followed by alkylation with iodoacetamide (Sigma Life Science) added to a final concentration of 30 mM and incubation for 15 min in darkness. Proteins were then extracted from the precleared lysates by protein aggregation capture (Batth et al. 2019). Briefly, Sera-Mag beads (5 μl at 50 μg/μl) (GE Healthcare Life Sciences) were washed with liquid chromatography-mass spectrometry (LC-MS)-grade acetonitrile (ACN) (EMD Millipore Corp.) on a magnetic rack. Tubes were removed from the magnetic rack, and lysate was added and then adjusted to 70% ACN to induce protein aggregation onto beads. Samples were allowed to settle for 10 min, gently resuspended, and allowed to settle for another 10 min. The samples were placed on a magnetic rack and the supernatant was removed, followed by washing with 1 ml of ACN and 1 ml of 70% ethanol (EMD Millipore Corp.) while on a magnetic rack. The samples were removed from the magnetic rack and 50 μl of Tris buffer was added. Proteins bound to beads were processed with two sequential aliquots of sequencing-grade trypsin (Thermo-Scientific) for an overnight and 3-h enzymatic digest using a 1:75 (wt/wt) protein/trypsin ratio at 37°C with constant

agitation (1,000 rpm). The samples were then adjusted to 0.1 % formic acid (FA) (Fisher Chemical), vortexed, and allowed to sit for 10 min. The samples were placed on a magnetic rack and supernatants containing the peptides were added to prewet Vivaspin 10 kDa MWCO filters (Sartorius) and centrifuged at 12,000 × *g* for 15 min at room temperature. Tryptic peptide flowthroughs were collected, and peptide concentrations were measured using the Nanodrop One spectrophotometer (Thermo-Scientific) and transferred to the autosampler vials for LC tandem MS (MS/MS) measurement.

Note that the root wash extraction described above was performed on a sample collected 48 h postinoculation ($n = 3$) with the 10-member SynCom and this measurement was paired with a "whole root plug" extract that is described below. These paired samples facilitated a metaproteomics comparison between microbiomes adhered to the root (i.e., root wash) versus those in close proximity (i.e., agar plug) (discussed above).

Extracting microbiomes from agar for metaproteomics.

Microbial cell populations in agar were selectively excised using a sterilized scalpel to assess microbiome changes in composition and function across time and in response to the plant root system. To characterize how the SynCom microbiome changes across time in the absence of a plant root system, agar plugs were obtained from culture plates that lacked a plant root system at 0 h (control plug 0 h), 24 h (control plug 24 h), and 48 h (control plug 48 h) in biological triplicate. Note, because the amount of microbial cells surrounding a plant root system are expected to change for different plant hosts and starting inocula, the size (i.e., volume) of the agar plug should be evaluated per biological system. In this study, agar plugs equivalent to 0.5 ml were sufficient for each sample and, thus, used throughout this study. The agar plugs obtained at 0 h were excised immediately after the media turned into a semisolid state in order to assess whether extractions from agar alter microbiome measurements when compared with those obtained from the starting SynCom inoculum. The SynCom liquid control stock sample was prepared in biological triplicate by washing pelleted cells with phosphate-buffered saline to remove media and resuspending cells in 100 mM ammonium bicarbonate.

For plant-agar cultures, agar plugs were excised to obtain four spatial measurements: whole root, root tip, root base, and a region distant from the plant root system (approximately 3 to 4 cm distant from root, near the edges of the Petri dish). Whole-root agar plug samples were collected at 48 h and the other locations were collected at 24 and 48 h in biological triplicate. To ensure sufficient material for subsequent extractions, multiple agar plugs were pooled together; for example, agar plugs from all root tips for each plant were pooled. Prior to additional sample processing, all agar plugs (0.5 ml) were liquified by heating for 10 min at 90°C in a heat block.

Samples were processed by adding an equal volume of lysis buffer (4% sodium deoxycholate [SDC] in 100 mM ammonium bicarbonate) (Sigma-Aldrich) to bring the final concentration to 2% SDC and kept warm to avoid solidification of agar. Note, SDC was selected as the detergent because, unlike SDS, it permits trypsin activity and is easily removed (Masuda et al. 2008). The samples were sonicated (30% amplitude, 10-s pulse with 10-s rest, 2-min total pulse time) (Branson digital sonifier), then incubated at 90°C for 10 min. The cell lysates were centrifuged at 21,000 × *g* for 10 min at room temperature to remove any cell debris and proteins were quantified with a Nanodrop One spectrophotometer (Thermo-Scientific). Samples were reduced and alkylated as described in the section above. Samples were

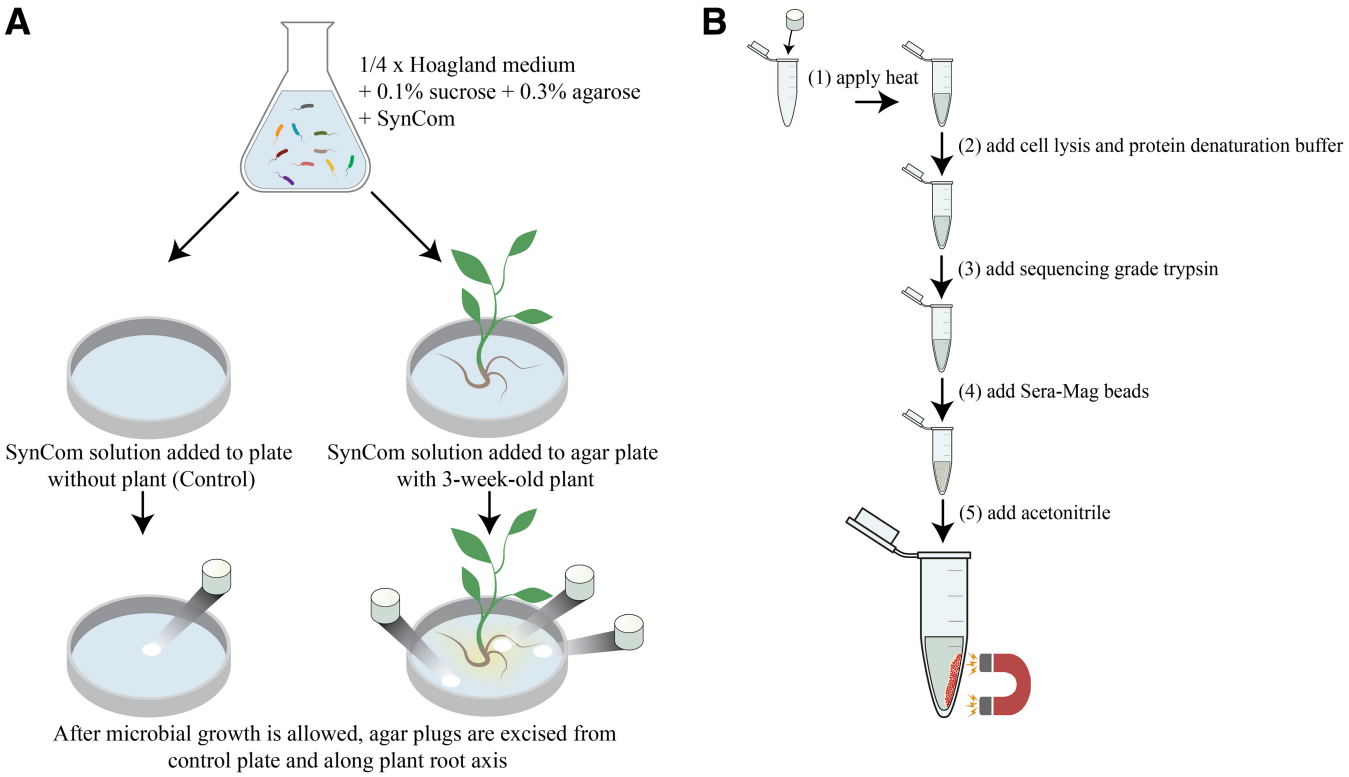

Fig. 5. Experimental design to achieve spatially resolved plant root-associated microbes using an agar system. **A,** A synthetic community (SynCom) containing 10 bacterial strains in equal numbers inoculated in 1/4× Hoagland's media + 0.1% sucrose + 0.3% agarose; control agar plates containing SynCom without a plant; plant (*Populus trichocarpa* B819) in agar containing SynCom; agar plugs excised from control agar plates containing SynCom without plant at 0, 24, and 48 h ($n = 3$); and agar plugs excised from root base, root tip, and distant regions for each plant in agar containing SynCom at 24 and 48 h ($n = 3$). **B,** In-solution cell lysis, enzymatic protein digestion, and peptide extraction using Sera-Mag beads.

heated again briefly to reliquify the agar and allowed to cool down; then, proteins were processed with two sequential aliquots of sequencing-grade trypsin for an overnight and 3-h enzymatic digest using a 1:75 (wt/wt) protein/trypsin ratio at 37°C with constant shaking (1,000 rpm). Each sample was acidified with 1% FA, vortexed, and centrifuged at maximum speed for 10 min at room temperature to precipitate and remove SDC. Samples were transferred to new Eppendorf tubes where Sera-Mag beads (GE Healthcare Life Sciences) were used to aggregate and remove the agar from the samples. For each sample, Sera-Mag beads (approximately 5 µl at 50 µg/µl, previously washed and resuspended in equal volume of ACN) were added and final volumes were adjusted to 70% LC-MS-grade acetonitrile (EMD Millipore Corp.). Twice, samples were vortexed gently and allowed to rest for 10 min to allow for aggregation of the agar matrix onto the magnetic beads. Eppendorf tubes were then transferred to a magnetic rack where the supernatant solution containing peptides was removed and subsequently transferred to new tubes (Fig. 5B). Importantly, care was taken to not aspirate Sera-Mag beads. To remove residual SDC, hydrated ethyl acetate was added to each sample at a 1:1 (vol/vol) ratio, vortexed, and centrifuged for 10 min at maximum speed. The lower aqueous layer containing the peptides was collected and cleaned again with ethyl acetate. The final lower aqueous layer containing peptides was transferred into new Eppendorf tubes, then vacuum-dried to completion using a SpeedVac Concentrator (Thermo-Fischer Scientific). The peptides were resolubilized in 0.1% trifluoroacetic acid and cleaned on a Pierce peptide desalting spin column (Thermo Scientific) per the manufacturer's instructions. Concentrated peptides were resuspended in a 25-µl aqueous solution (0.1% FA) and subsequently quantified using a Nanodrop One spectrophotometer (Thermo Scientific). Peptides were transferred to autosampler vials for LC-MS/MS measurements.

Protein identification and quantification.

All peptides were analyzed using two-dimensional LC on an Ultimate 3000 RSLCnano system (Thermo-Fisher Scientific) coupled with a Q Exactive Plus mass spectrometer (Thermo-Fisher Scientific). For each sample, a 2-µg inject of digested peptide mixture was flowed across an in-house-built strong cation exchange (SCX) Luna trap column (5 µm by 150 µm by 50 mm) (Phenomenex) followed by a nanoEase symmetry reversed-phase (RP) C18 trap column (5 µm by 300 µm by 50 mm) (Waters) and an aqueous solvent (5% ACN and 0.1% FA), then washed for 10 min. The loaded peptide mixtures were separated and analyzed across three successive SCX fractions of increasing concentrations of ammonium acetate (35 mM, 50 mM, and 1 M), each followed by a 100-min linear organic gradient (250 nl/min flow rate) from 5% aqueous solvent (5% ACN and 0.1% FA) to 30% organic solvent (80% ACN and 0.1% FA) to separate peptides across an in-house-pulled nanospray emitter (75 µm by 350 mm) packed with C18 Kinetex RP C18 resin (1.7 µm) (Phenomenex). All MS data were acquired with Thermo Xcalibur (version 4.2.47) using the top N method, where N could be up to 10. Target values for the full-scan MS spectra were 3×10^6 charges in the 300 to 1,500 m/z range with a maximum injection time of 25 ms. Transient times corresponding to a resolution of 70,000 at m/z 200 were chosen. A 1.6 m/z isolation window and fragmentation of precursor ions was performed by higher-energy C-trap dissociation with a normalized collision energy of 27 eV. MS/MS scans were performed at a resolution of 17,500 at m/z 200 with an ion target value of 1×10^5 and a 50-ms maximum injection time. Dynamic exclusion was set to 20 s to avoid repeated sequencing of peptides. All MS raw data files were analyzed using the Proteome Discoverer software (version 2.5) (Thermo-Fisher Scientific) (Orsburn 2021). Each MS raw data file was processed by the SEQUEST HT database search algorithm (Eng et al. 1994) and confidence in peptide-to-spectrum (PSM) matching was evaluated by Percolator (Kall et al. 2007). Peptide and PSMs were considered identified at $q < 0.01$ and proteins were required to have at least one unique peptide sequence. Protein relative abundance values were calculated by summing together peptide extracted ion chromatograms. Organism relative abundances were calculated by dividing their summed protein abundances from the sum total of all quantified protein abundances (Kleiner et al. 2017; Shrestha et al. 2021).

Statistical analysis.

Proteins with at least one unique peptide were exported from Proteome Discoverer. Log_2-transformation of protein abundances was performed followed by local regression (LOESS) normalization and mean-centering across the entire dataset using InfernoRDN software (v1.1.7793) (Polpitiya et al. 2008). To identify the differences in the proteome expression of the bacteria between different sample groups, PERMANOVA was performed across the control, distant from root, root tip, and root base samples at 24- and 48-h time points using the vegan package (v.2.5-7) in R (Oksanen 2020). Protein abundances subset for each bacterial strain of the SynCom were extracted from the normalized dataset and further mean-centered using InfernoRDN. To improve the robustness of downstream analysis, the analysis was limited to proteins that were identified in at least two of three replicates of at least one sample group. The abundance values for proteins with missing values were imputed with random values drawn from the normal distribution (width 0.3, downshift 2.8) using Perseus software (v.1.6.12.0) (Tyanova et al. 2016). To identify the proteins that are differentially expressed across the measured proteomes, ANOVA was performed (permutation-based false discovery rate [FDR] < 0.05; number of randomizations = 250) across experimental conditions. Proteins that passed the significance threshold of P value ≤ 0.05 were characterized as significantly differentially abundant. One-way hierarchical clustering of standardized Z-scores using Euclidean distances for rows was performed for significantly changing proteins. For the clusters obtained, GO enrichment tests were performed using a Fischer's exact test using the OmicsBox software tool (v.1.4.11). Biological process and molecular function GO terms that had an FDR-controlled P value < 0.05 were considered enriched.

Data availability.

All proteomics spectral data in this study were deposited at the ProteomeXchange Consortium via the MASSIVE repository. The ProteomeXchange project identifier is PXD030409 and the MassIVE identified is MSV000088566.

AUTHOR-RECOMMENDED INTERNET RESOURCES

DOE Public Access Plan: http://energy.gov/downloads/doe-public-access-plan
MASSIVE repository: https://massive.ucsd.edu/
OmicsBox software tool: https://www.biobam.com/omicsbox
Plant-Microbe Interfaces Scientific Focus Area: http://pmi.ornl.gov
vegan package in R: https://CRAN.R-project.org/package=vegan

LITERATURE CITED

Abreu, N. A., and Taga, M. E. 2016. Decoding molecular interactions in microbial communities. FEMS Microbiol. Rev. 40:648-663.

Aufrecht, J. A., Timm, C. M., Bible, A., Morrell-Falvey, J. L., Pelletier, D. A., Doktycz, M. J., and Retterer, S. T. 2018. Quantifying the spatiotemporal dynamics of plant root colonization by beneficial bacteria in a microfluidic habitat. Adv. Biosyst. 2:1-12.

Bais, H. P., Broeckling, C. D., and Vivanco, J. M. 2008. Root exudates modulate plant–microbe interactions in the rhizosphere. Pages 241-252 in: Secondary Metabolites in Soil Ecology. P. Karlovsky, ed. Springer, Berlin Heidelberg, Germany.

Bao, Z. H., Okubo, T., Kubota, K., Kasahara, Y., Tsurumaru, H., Anda, M., Ikeda, S., and Minamisawa, K. 2014. Metaproteomic identification of diazotrophic methanotrophs and their localization in root tissues of field-grown rice plants. Appl. Environ. Microbiol. 80:5043-5052.

Batth, T. S., Tollenaere, M. X., Ruther, P., Gonzalez-Franquesa, A., Prabhakar, B. S., Bekker-Jensen, S., Deshmukh, A. S., and Olsen, J. V. 2019. Protein aggregation capture on microparticles enables multipurpose proteomics sample preparation. Mol. Cell. Proteomics 18: 1027-1035.

Bible, A. N., Fletcher, S. J., Pelletier, D. A., Schadt, C. W., Jawdy, S. S., Weston, D. J., Engle, N. L., Tschaplinski, T., Masyuko, R., Polisetti, S., Bohn, P., Coutinho, T. A., Doktycz, M. J., and Morrell-Falvey, J. L. 2016. A carotenoid-deficient mutant in *Pantoea* sp. YR343, a bacteria isolated from the rhizosphere of *Populus deltoides*, is defective in root colonization. Front. Microbiol. 7:491.

Blair, P. M., Land, M. L., Piatek, M. J., Jacobson, D. A., Lu, T. Y. S., Doktycz, M. J., and Pelletier, D. A. 2018. Exploration of the biosynthetic potential of the *Populus* microbiome. mSystems 3:e00045-18.

Bona, E., Massa, N., Novello, G., Boatti, L., Cesaro, P., Todeschini, V., Magnelli, V., Manfredi, M., Marengo, E., Mignone, F., Berta, G., Lingua, G., and Gamalero, E. 2019. Metaproteomic characterization of the *Vitis vinifera* rhizosphere. FEMS Microbiol. Ecol. 95:fiy204.

Bonkowski, M., Tarkka, M., Razavi, B. S., Schmidt, H., Blagodatskaya, E., Koller, R., Yu, P., Knief, C., Hochholdinger, F., and Vetterlein, D. 2021. Spatiotemporal dynamics of maize (*Zea mays* L.) root growth and its potential consequences for the assembly of the rhizosphere microbiota. Front. Microbiol. 12:619499.

Brown, S. D., Utturkar, S. M., Klingeman, D. M., Johnson, C. M., Martin, S. L., Land, M. L., Lu, T. Y. S., Schadt, C. W., Doktycz, M. J., and Pelletier, D. A. 2012. Twenty-one genome sequences from pseudomonas species and 19 genome sequences from diverse bacteria isolated from the rhizosphere and endosphere of *Populus deltoides*. J. Bacteriol. 194: 5991-5993.

Carper, D. L., Weston, D. J., Barde, A., Timm, C. M., Lu, T. Y., Burdick, L. H., Jawdy, S. S., Klingeman, D. M., Robeson, M. S., 2nd, Veach, A. M., Cregger, M. A., Kalluri, U. C., Schadt, C. W., Podar, M., Doktycz, M. J., and Pelletier, D. A. 2021. Cultivating the bacterial microbiota of *Populus* roots. mSystems 6:e0130620.

Chiu, C. Y., Wang, M. K., Hwong, J. L., and King, H. B. 2002. Physical and chemical properties in rhizosphere and bulk soils of Tsuga and Yushania in a temperate rain forest. Commun. Soil Sci. Plant Anal. 33: 1723-1735.

Chourey, K., Jansson, J., VerBerkmoes, N., Shah, M., Chavarria, K. L., Tom, L. M., Brodie, E. L., and Hettich, R. L. 2010. Direct cellular lysis/protein extraction protocol for soil metaproteomics. J. Proteome Res. 9: 6615-6622.

Dennis, P. G., Miller, A. J., and Hirsch, P. R. 2010. Are root exudates more important than other sources of rhizodeposits in structuring rhizosphere bacterial communities? FEMS Microbiol. Ecol. 72:313-327.

Doornbos, R. F., van Loon, L. C., and Bakker, P. A. H. M. 2012. Impact of root exudates and plant defense signaling on bacterial communities in the rhizosphere. A review. Agron. Sustainable Dev. 32:227-243.

Eng, J. K., McCormack, A. L., and Yates, J. R. 1994. An approach to correlate tandem mass spectral data of peptides with amino acid sequences in a protein database. J. Am. Soc. Mass. Spectrom. 5:976-989.

Estenson, K., Hurst, G. B., Standaert, R. F., Bible, A. N., Garcia, D., Chourey, K., Doktycz, M. J., and Morrell-Falvey, J. L. 2018. Characterization of Indole-3-acetic acid biosynthesis and the effects of this phytohormone on the proteome of the plant-associated microbe *Pantoea* sp. YR343. J. Proteome Res. 17:1361-1374.

Goldford, J. E., Lu, N., Bajic, D., Estrela, S., Tikhonov, M., Sanchez-Gorostiaga, A., Segre, D., Mehta, P., and Sanchez, A. 2018. Emergent simplicity in microbial community assembly. Science 361:469-474.

Hara, S., Morikawa, T., Wasai, S., Kasahara, Y., Koshiba, T., Yamazaki, K., Fujiwara, T., Tokunaga, T., and Minamisawa, K. 2019. Identification of nitrogen-fixing bradyrhizobium associated with roots of field-grown sorghum by metagenome and proteome analyses. Front. Microbiol. 10:407.

Hasim, S., Allison, D. P., Mendez, B., Farmer, A. T., Pelletier, D. A., Retterer, S. T., Campagna, S. R., Reynolds, T. B., and Doktycz, M. J. 2018. Elucidating duramycin's bacterial selectivity and mode of action on the bacterial cell envelope. Front. Microbiol. 9:219.

Hemkemeyer, M., Pronk, G. J., Heister, K., Kogel-Knabner, I., Martens, R., and Tebbe, C. C. 2014. Artificial soil studies reveal domain-specific preferences of microorganisms for the colonisation of different soil minerals and particle size fractions. FEMS Microbiol. Ecol. 90:770-782.

Hirsch, P. R., and Mauchline, T. H. 2012. Who's who in the plant root microbiome? Nat. Biotechnol. 30:961-962.

Iijima, M., Griffiths, B., and Bengough, A. G. 2000. Sloughing of cap cells and carbon exudation from maize seedling roots in compacted sand. New Phytol. 145:477-482.

Kall, L., Canterbury, J. D., Weston, J., Noble, W. S., and MacCoss, M. J. 2007. Semi-supervised learning for peptide identification from shotgun proteomics datasets. Nat. Methods 4:923-925.

Kleiner, M., Thorson, E., Sharp, C. E., Dong, X., Liu, D., Li, C., and Strous, M. 2017. Assessing species biomass contributions in microbial communities via metaproteomics. Nat. Commun. 8:1558.

Knee, E. M., Gong, F. C., Gao, M. S., Teplitski, M., Jones, A. R., Foxworthy, A., Mort, A. J., and Bauer, W. D. 2001. Root mucilage from pea and its utilization by rhizosphere bacteria as a sole carbon source. Mol. Plant-Microbe Interact. 14:775-784.

Knief, C., Delmotte, N., Chaffron, S., Stark, M., Innerebner, G., Wassmann, R., von Mering, C., and Vorholt, J. A. 2012. Metaproteogenomic analysis of microbial communities in the phyllosphere and rhizosphere of rice. ISME J. 6:1378-1390.

Kumar, S. V., Abraham, P. E., Hurst, G. B., Chourey, K., Bible, A. N., Hettich, R. L., Doktycz, M. J., and Morrell-Falvey, J. L. 2020. A carotenoid-deficient mutant of the plant-associated microbe *Pantoea* sp. YR343 displays an altered membrane proteome. Sci. Rep. 10:14985.

Levy, A., Gonzalez, I. S., Mittelviefhaus, M., Clingenpeel, S., Paredes, S. H., Miao, J. M., Wang, K. R., Devescovi, G., Stillman, K., Monteiro, F., Alvarez, B. R., Lundberg, A. D. S., Lu, T. Y., Lebeis, S., Jin, Z., McDonald, M., Klein, A. P., Feltcher, M. E., Rio, T. G., and Dangl, J. L. 2018. Genomic features of bacterial adaptation to plants. Nat. Genet. 50:138.

Long, S., Yang, Y., Shen, C., Wang, Y., Deng, A., Qin, Q., and Qiao, L. 2020. Metaproteomics characterizes human gut microbiome function in colorectal cancer. NPJ Biofilms Microbiomes 6:14.

Mandalakis, M., Panikov, N. S., Polymenakou, P. N., Sizova, M. V., and Stamatakis, A. 2018. A simple cleanup method for the removal of humic substances from soil protein extracts using aluminum coagulation. Environ. Sci. Pollut. Res. 25:23845-23856.

Masuda, T., Tomita, M., and Ishihama, Y. 2008. Phase transfer surfactant-aided trypsin digestion for membrane proteome analysis. J. Proteome Res. 7:731-740.

Mattarozzi, M., Di Zinno, J., Montanini, B., Manfredi, M., Marengo, E., Fornasier, F., Ferrarini, A., Careri, M., and Visioli, G. 2020. Biostimulants applied to maize seeds modulate the enzymatic activity and metaproteome of the rhizosphere. Appl. Soil Ecol. 148:103480.

Mattarozzi, M., Manfredi, M., Montanini, B., Gosetti, F., Sanangelantoni, A. M., Marengo, E., Careri, M., and Visioli, G. 2017. A metaproteomic approach dissecting major bacterial functions in the rhizosphere of plants living in serpentine soil. Anal. Bioanal. Chem. 409:2327-2339.

Mello, B. L., Alessi, A. M., McQueen-Mason, S., Bruce, N. C., and Polikarpov, I. 2016. Nutrient availability shapes the microbial community structure in sugarcane bagasse compost-derived consortia. Sci. Rep. 6:38781.

Munoz-Ucros, J., Zwetsloot, M. J., Cuellar-Gempeler, C., and Bauerle, T. L. 2021. Spatiotemporal patterns of rhizosphere microbiome assembly: From ecological theory to agricultural application. J. Appl. Ecol. 58:894-904.

Nobori, T., Wang, Y., Wu, J., Stolze, S. C., Tsuda, Y., Finkemeier, I., Nakagami, H., and Tsuda, K. 2020. Multidimensional gene regulatory landscape of a bacterial pathogen in plants. Nat. Plants 6: 883-896.

O'Banion, B. S., O'Neal, L., Alexandre, G., and Lebeis, S. L. 2020. Bridging the gap between single-strain and community-level plant-microbe chemical interactions. Mol. Plant-Microbe Interact. 33:124-134.

Oksanen, J., Blanchet, F. G., Friendly, M., Kindt, R., Legendre, P., McGlinn, D., Minchin, P., O'Hara, R. B., Simpson, G. L., Solymos, P., Stevens, M. H. H., Szöcs, E., and Wagner, H. H. 2020. vegan community ecology package version 2.5-7.

Orsburn, B. C. 2021. Proteome discoverer-a community enhanced data processing suite for protein informatics. Proteomes 9:15.

Polpitiya, A. D., Qian, W. J., Jaitly, N., Petyuk, V. A., Adkins, J. N., Camp, D. G., 2nd, Anderson, G. A., and Smith, R. D. 2008. DAnTE: A statistical tool for quantitative analysis of -omics data. Bioinformatics 24:1556-1558.

Poole, P. 2017. Shining a light on the dark world of plant root-microbe interactions. Proc. Nat. Acad. Sci. U.S.A. 114:4281-4283.

Qian, C., and Hettich, R. L. 2017. Optimized extraction method to remove humic acid interferences from soil samples prior to microbial proteome measurements. J. Proteome Res. 16:2537-2546.

Ramirez-Villacis, D. X., Finkel, O. M., Salas-Gonzalez, I., Fitzpatrick, C. R., Dangl, J. L., Jones, C. D., and Leon-Reyes, A. 2020. Root microbiome modulates plant growth promotion induced by low doses of glyphosate. mSphere 5:e00484-20.

Reasoner, D. J., and Geldreich, E. E. 1985. A new medium for the enumeration and subculture of bacteria from potable water. Appl. Environ. Microbiol. 49:1-7.

Renu, Gupta, S. K., Rai, A. K., Sarim, K. M., Sharma, A., Budhlakoti, N., Arora, D., Verma, D. K., and Singh, D. P. 2019. Metaproteomic data of maize rhizosphere for deciphering functional diversity. Data Brief. 27:104574.

Ruger, L., Feng, K., Dumack, K., Freudenthal, J., Chen, Y., Sun, R. B., Wilson, M., Yu, P., Sun, B., Deng, Y., Hochholdinger, F., Vetterlein, D., and Bonkowski, M. 2021. Assembly patterns of the rhizosphere microbiome along the longitudinal root axis of maize (*Zea mays* L.). Front. Microbiol. 12:614501.

Schaefer, A. L., Lappala, C. R., Morlen, R. P., Pelletier, D. A., Lu, T. Y. S., Lankford, P. K., Harwood, C. S., and Greenberg, E. P. 2013. LuxR- and LuxI-type quorum-sensing circuits are prevalent in members of the *Populus deltoides* microbiome. Appl. Environ. Microbiol. 79: 5745-5752.

Schirawski, J., and Perlin, M. H. 2018. Plant(-)Microbe interaction 2017-the good, the bad and the diverse. Int. J. Mol. Sci. 19:1374.

Sharma, S., Mehta, R., Gupta, R., and Schloter, M. 2012. Improved protocol for the extraction of bacterial mRNA from soils. J. Microbiol. Methods 91:62-64.

Shrestha, H. K., Appidi, M. R., Villalobos Solis, M. I., Wang, J., Carper, D. L., Burdick, L., Pelletier, D. A., Doktycz, M. J., Hettich, R. L., and Abraham, P. E. 2021. Metaproteomics reveals insights into microbial structure, interactions, and dynamic regulation in defined communities as they respond to environmental disturbance. BMC Microbiol. 21: 308.

Shrestha, S., and Kafle, G. 2020. Variation of selected physicochemical and hydrological properties of soils in different tropical land use systems of Nepal. Appl. Environ. Soil Sci. 2020:8877643.

Tartaglia, M., Bastida, F., Sciarrillo, R., and Guarino, C. 2020. Soil metaproteomics for the study of the relationships between microorganisms and plants: A review of extraction protocols and ecological insights. Int. J. Mol. Sci. 21:8455.

Tecon, R., Mitri, S., Ciccarese, D., Or, D., van der Meer, J. R., and Johnson, D. R. 2019. Bridging the holistic-reductionist divide in microbial ecology. mSystems 4:e00265-18.

Timm, C. M., Pelletier, D. A., Jawdy, S. S., Gunter, L. E., Henning, J. A., Engle, N., Aufrecht, J., Gee, E., Nookaew, I., Yang, Z. M., Lu, T. Y., Tschaplinski, T. J., Doktycz, M. J., Tuskan, G. A., and Weston, D. J. 2016. Two poplar-associated bacterial isolates induce additive favorable responses in a constructed plant-microbiome system. Front. Plant Sci. 7:497.

Tyanova, S., Temu, T., Sinitcyn, P., Carlson, A., Hein, M. Y., Geiger, T., Mann, M., and Cox, J. 2016. The Perseus computational platform for comprehensive analysis of (prote)omics data. Nat. Methods 13:731-740.

Vandenkoornhuyse, P., Quaiser, A., Duhamel, M., Le Van, A., and Dufresne, A. 2015. The importance of the microbiome of the plant holobiont. New Phytol. 206:1196-1206.

Walker, T. S., Bais, H. P., Grotewold, E., and Vivanco, J. M. 2003. Root exudation and rhizosphere biology. Plant Physiol. 132:44-51.

Wang, J., Carper, D. L., Burdick, L. H., Shrestha, H. K., Appidi, M. R., Abraham, P. E., Timm, C. M., Hettich, R. L., Pelletier, D. A., and Doktycz, M. J. 2021. Formation, characterization and modeling of emergent synthetic microbial communities. Comput. Struct. Biotechnol. J. 19:1917-1927.

Yee, M. O., Kim, P., Li, Y. F., Singh, A. K., Northen, T. R., and Chakraborty, R. 2021. Specialized plant growth chamber designs to study complex rhizosphere interactions. Front. Microbiol. 12:625752.

Zengler, K., Hofmockel, K., Baliga, N. S., Behie, S. W., Bernstein, H. C., Brown, J. B., Dinneny, J. R., Floge, S. A., Forry, S. P., Hess, M., Jackson, S. A., Jansson, C., Lindemann, S. R., Pett-Ridge, J., Maranas, C., Venturelli, O. S., Wallenstein, M. D., Shank, E. A., and Northen, T. R. 2019. EcoFABs: Advancing microbiome science through standardized fabricated ecosystems. Nat. Methods 16:567-571.